COLLÈGE DE FRANCE
Laboratoire de Physique Corpusculaire

MEASUREMENT OF **EMI** AND **HAMAMATSU** PHOTOMULTIPLIER CHARACTERISTICS FOR THE **CHOOZ** EXPERIMENT

P. Salin, S. Sukhotin

COLLEGE DE FRANCE, IN2P3-CNRS, Laboratoire de Physique Corpusculaire,
11 Place Marcelin Berthelot, F-75231 Paris Cedex 05, FRANCE

Measurement of EMI and HAMAMATSU photomultiplier characteristics for the CHOOZ experiment.

P. Salin[1] and S. Sukhotin[2]

---

[1] Collège de France.
[2] Kourchatov Institute, visitor at Collège de France.

Measurement of EMI and HAMAMATSU photomultiplier characteristics.

1. Introduction

This work was done in the framework of the future CHOOZ experiment to search for neutrino oscillation at a distance of 1 km from a nuclear reactor. The detector design is shown on figure 1. The proposal of the CHOOZ experiment[1] rests on using a large liquid scintillator detector in the center part of which gadolinium-loaded scintillator will be used. Antineutrinos from nuclear reactors will be detected via the reaction :

$$\bar{\nu}_e + p \rightarrow e^+ + n$$
$$\lfloor + Gd \rightarrow \gamma_1 , \gamma_2... + <E> = 8 \text{ MeV}$$
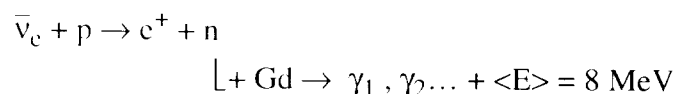
with a neutron lifetime in the gadolinium scintillator of about 28 µs.

The fiducial volume is viewed by 160 photomultipliers (PM) which give the information about the energy of e^+ and n events as well as the time delay between these two. The time and energy balance information will provide a localisation of an event.

Monte-Carlo calculations[2] of efficiency and light collection parameters of the detector showed that we have for the $e^\pm$ 150 photo-electrons/event at E≈ 1 MeV. It means that individual PMs will operate in single photoelectron regime. So, the PM parameters in this regime are very important and the Chooz collaboration needs to find good PM with best peak-to-valley ratio, low dark current counting rate etc. The Collège de France group is preparing a Flash ADC electronics, to sample the PM pulses[3]. The results of the present test will be a part of a full PM+FADC test to be installed in the laboratory in a near future.

Many types of PM have been already checked in other laboratories (see for example [4,5]). We selected THORN-EMI-9351 and HAMAMATSU (R4558) 8" phototubes.
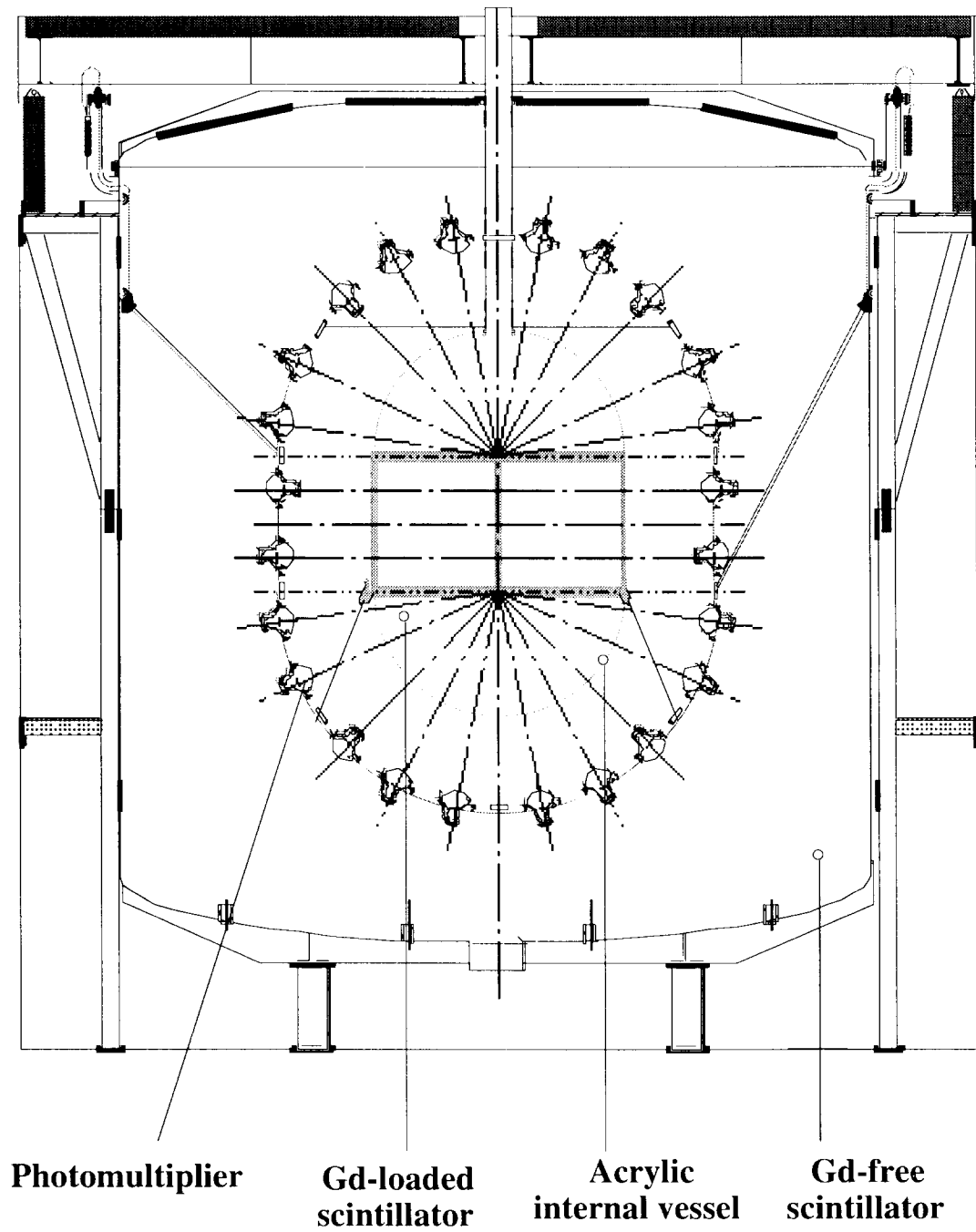
The followings characteristics have been investigated for both PM:

- Shape of single-electron anode pulse.
- Single-electron transit time distribution.
- Afterpulses.
- Dark-current rate.

With EMI-9351 the time characteristic for CHOOZ regular and gadolinium-loaded scintillators were measured with a ^{207}Bi source (EC with E = 976 keV).

2. Description of the electronic set-up :

For EMI-9351 we used the divider-type B[6] with two independent high voltage power supplies: one for the photocathode and another one for all dynodes. So, we could vary independently the potential between photocathode and the first dynode and the potential between first dynode and the ground, according to figure 2.

**Photomultiplier   Gd-loaded   Acrylic   Gd-free
                     scintillator   internal vessel scintillator**

The CHOOZ experiment Neutrino Detector

Figure 1.

Photocathode (pc)

d1 d2 d3 d4 d5 d6 d7 d8 d9 d10 d11 d12

Anode

R1 R2 R3 R4 R5 R6 R7 R8 R9 R10 R11 R12

Ra

1nF 1nF 1nF

HV2

HV1

$1400 \text{ V} \leq HV1 \leq 1800 \text{ V}$
$950 \text{ V} \leq HV2 \leq 1200 \text{ V}$

$R1 = R2 = 305 \text{ k}\Omega$

$R3 = ... = R8 = 161 \text{ k}\Omega$

$R9 = 235 \text{ k}\Omega$; $R10 = 330 \text{ k}\Omega$

$R11 = 487 \text{ k}\Omega$

$R12 = 630 \text{ k}\Omega$

$Ra = 10 \text{ k}\Omega$
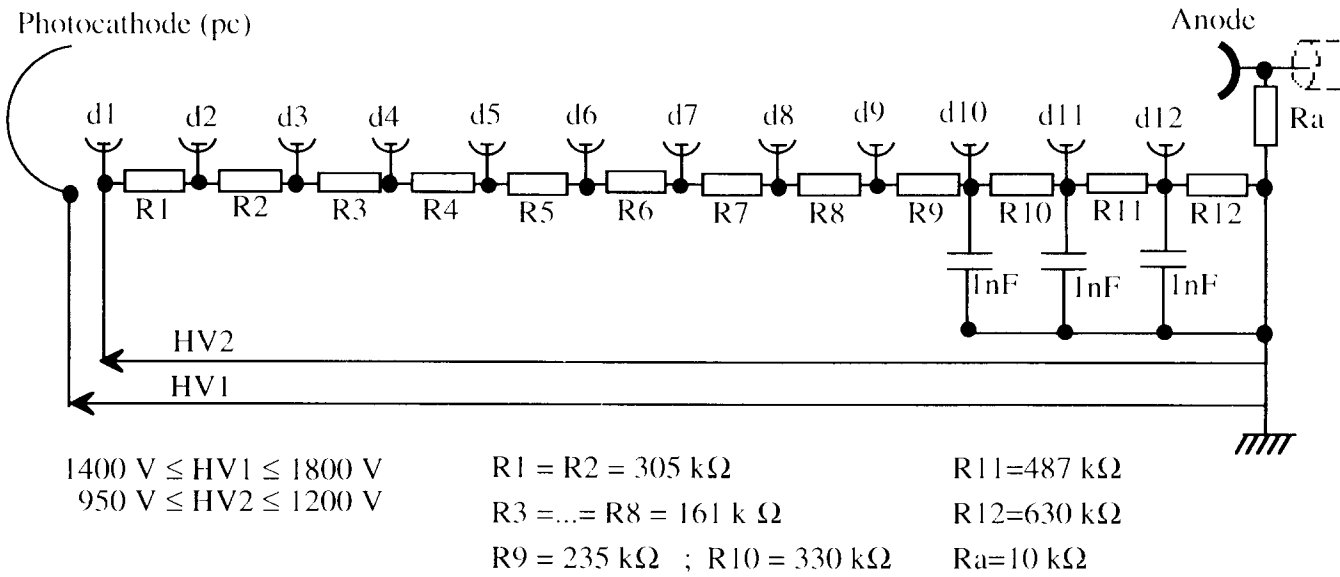
Figure 2 : High voltage divider-type B for EMI.

For EMI we varied the voltage between the photocathode and first dynode-V(pc -d1) and the voltage between first dynode and ground-V(d1-grnd) in wide ranges, which are indicated on figure 2. For HAMAMATSU the standard resistor divider, recommended by the firm, was used.
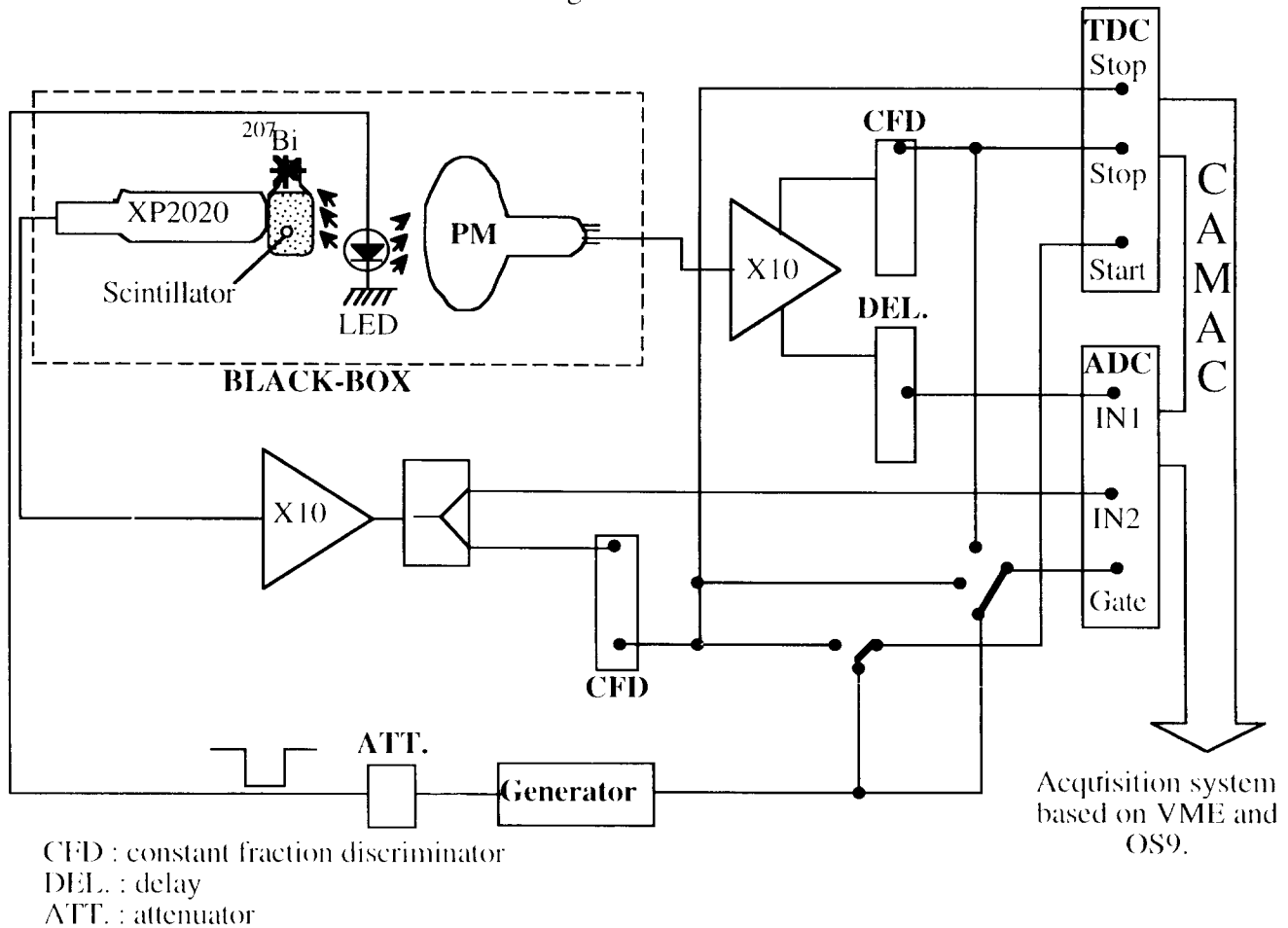
The electronic scheme is shown in figure 3.

TDC
Stop

CFD

Stop

Start

^{207}Bi

XP2020

Scintillator

LED

PM

X10

DEL.

ADC
IN1

CAMAC

BLACK-BOX

X10

CFD

IN2

Gate

ATT.

Generator

Acquisition system based on VME and OS9.

CFD : constant fraction discriminator
DEL. : delay
ATT. : attenuator

Figure 3 : Electronic scheme of the measurement set-up.

3. Single photo-electron charge spectrum.

The measurements of dark-current spectra for both PM were done after some days of keeping PM in darkness with high voltage applied as follow : V(pc-d1) = 550 V and V(d1-grnd) = 1050 V for EMI and V = 1675 V for HAMAMATSU. The dark-current rate after 48 hours in darkness was stable. At a threshold of 0.1 single photoelectron peak the counting rates were: for EMI $\approx$ 800 s^{1} and 1400 s^{1} for HAMAMATSU. The typical dark-current amplitude spectra (i.e. a number of events plot versus ADC channel) are shown in figure 4, for EMI and HAMAMATSU, just for demonstration the more interesting parameter of these spectra - a peak-to-valley ratio.

One can see an evident peak corresponding single-electron noise with a noise from dynodes in the left part of the charge distribution spectrum. HAMAMATSU behaves much worse than EMI, with bad peak-to-valley ratio. Taking this into account, more detailed measurements were done only with EMI-9351.

For EMI data, a fit was done to estimate the probability of emitting 2 or more photo-electrons in the dark current spectrum. The function fitted is the sum of an exponential function with parameters P1, P2 and two gaussians. Parameters P3, P4, P5 are for the first gaussian (P3 is the normalization constant, P4 is the mean value and P5 is the width). P6 is the normalization for the second gaussian with a mean value 2P4 and a width$\sqrt{2}$ P5. P7 is a value for the pedestal. The dark current spectrum and the fit are presented on figure 5. We estimate the contribution of 2 or more photo-electrons to be less than 3 % for the EMI-9351 photomultiplier in the dark current spectrum.

For the light source we used three kinds of LED (light-emitting diode) with different colours: red, green and yellow to make sure that the single photoelectron response does not depend on the light wave length. To obtain the shortest and fastest light pulse possible we polarized the LED in the avalanche mode i.e. in the forbidden polarity (negative) with a generator pulse. For some LED the slope of the characteristic is not steep enough , fortunately some present a very high slope (few A/V), with acceptable voltage pulse (a few tens volt).

To check that the generator pulse amplitude for the LED corresponds to a single-electron response from the PM the measurement with a long width of generator pulse (up to 450 ns) was done to see the expected plateau in time distribution. The result is presented in figure 6, with an amplitude distribution (top plot) and a time distribution (bottom plot). On the bottom plot, parameters of a linear fit are presented together with the fit, which is practically a constant.

The measurements with LED collected at the same time information from the ADC (to be sure that the PM is in the single-electron regime) and information from the TDC with transit time distribution. We went (step by step) through wide scale of potentials between photocathode and first dynode from 350 V up to 700 V, with a fixed potential between the first dynode and the ground (V(d1-grnd) = 1050 V). We present for six different values of the mentioned potential the following data: ADC distribution (fig. 7), TDC distribution for the main peak (fig. 8) and TDC distribution in a logarithmic scale (fig. 9) to demonstrate the deposit of afterpulses. Each bin in the TDC distributions equals 0.5 ns. Notice here, that for our measurements with a classical (start-stop) TDC, afterpulses correspond to the situation when a photoelectron was registered by TDC not within a main peak time window, but with some delay. In other words, sometimes a photoelectron transit time is bigger than the mean transit time. The results of these measurements were fitted. The following parameters: (mean peak position/width)^{2} and a peak-to-valley ratio for amplitude distribution, as well as the peak position and the width of the transit time distribution were determined and their dependence versus the voltage between photocathode and first dynode are plotted on figure10.
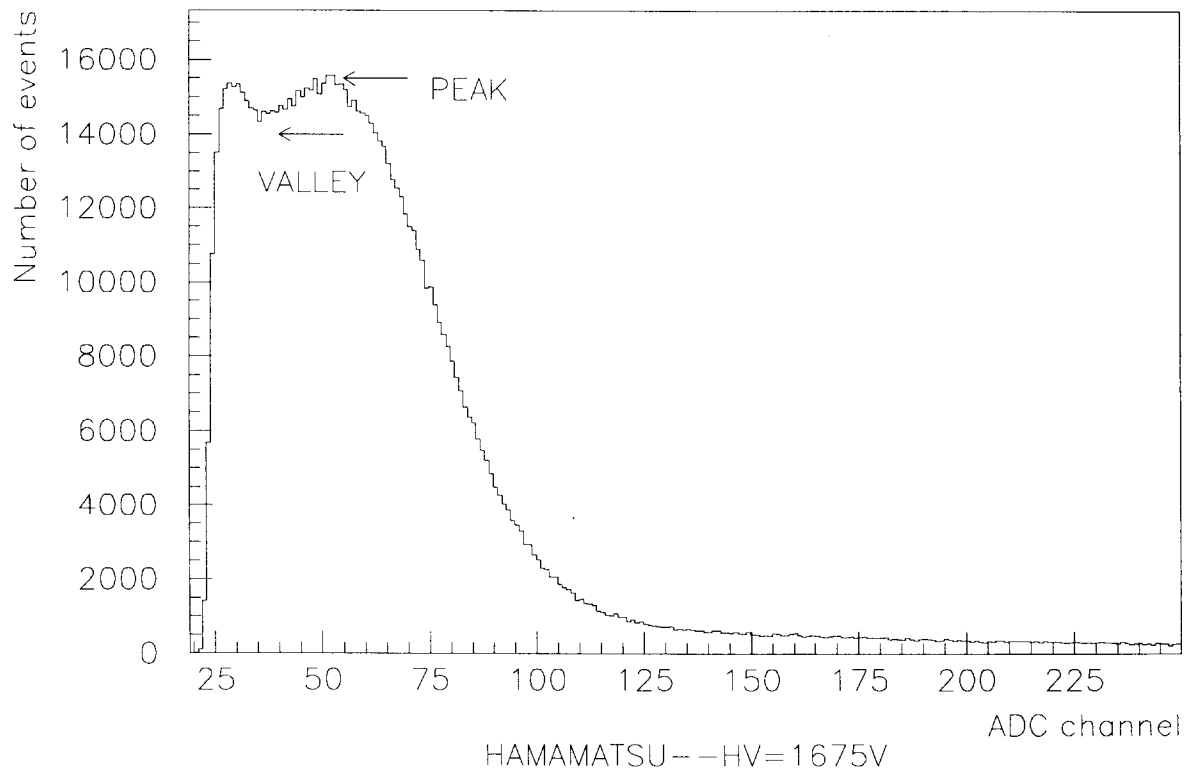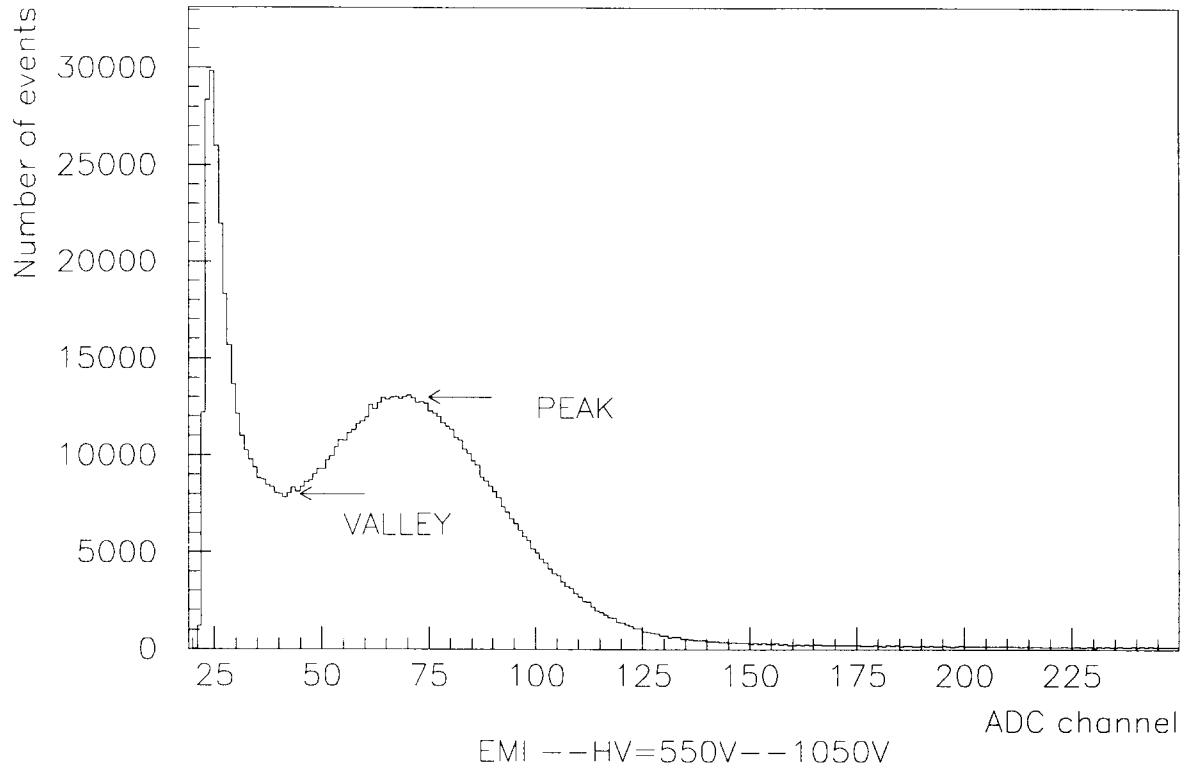
Figure 4 : Typical dark-current amplitude spectra.

Figure 5 : Fit for EMI dark-current spectrum.

EMI V(pc−d1)=550V V(d1−grnd)=1050V Neg.polarity yellow LED

ID	1
Entries	500000
Mean	19.95
RMS	5.320

Number of events

ADC channel

ADC − single PE spectrum

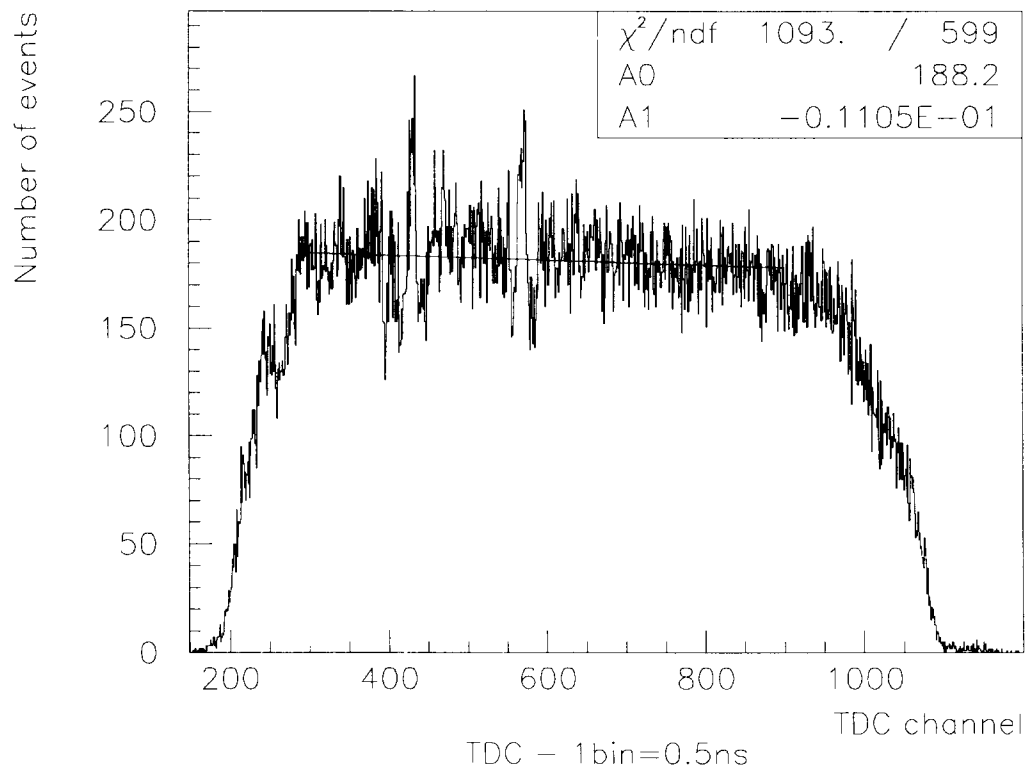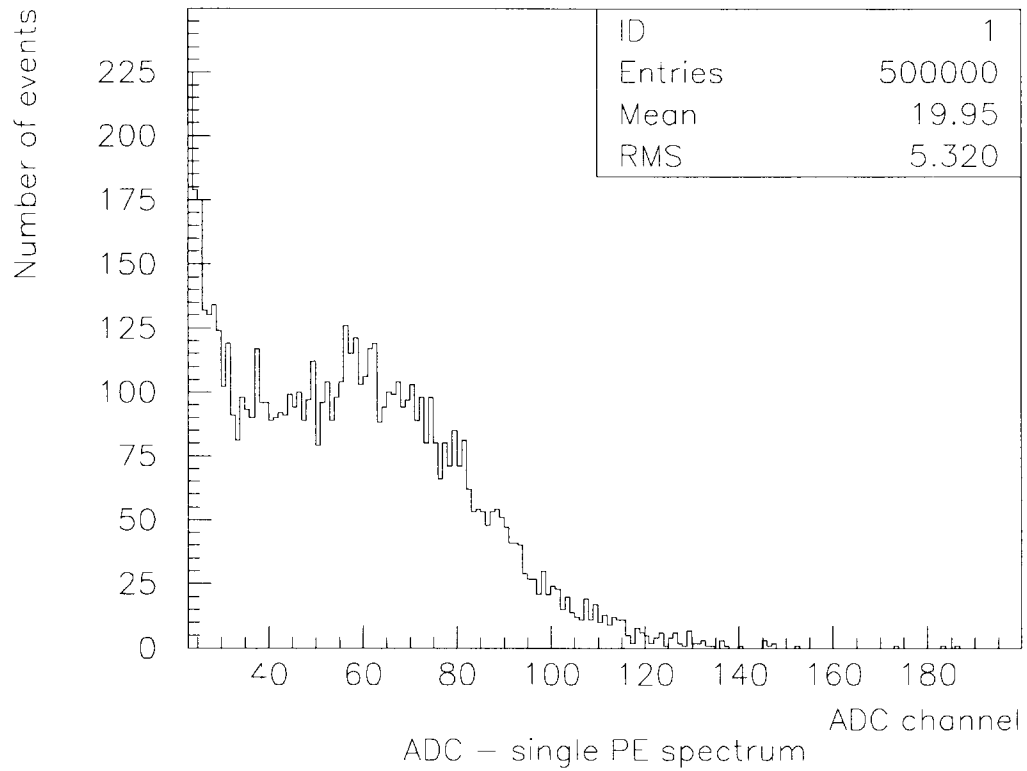| χ^2/ndf | 1093. / 599 |
| A0 | 188.2 |
| A1 | −0.1105E−01 |

Number of events

TDC channel

TDC − 1bin=0.5ns

Figure 6: ADC and TDC spectrum with a long width LED pulse.

8

Single PE spectra V(d1−grnd)=1050v.Diff.V(pc−d1).LED−−Neg.polar.

χ^2/ndf	71.70	/	53
Constant			1167.
Mean			57.49
Sigma			20.67

V(pc−d1)=350v

χ^2/ndf	64.32	/	53
Constant			1110.
Mean			64.21
Sigma			21.81

V(pc−d1)=450v

χ^2/ndf	501.0	/	78
Constant			8391.
Mean			66.47
Sigma			22.73

V(pc−d1)=525v

χ^2/ndf	34.90	/	53
Constant			2177.
Mean			70.90
Sigma			22.67

V(pc−d1)=550v

χ^2/ndf	62.42	/	63
Constant			1102.
Mean			72.79
Sigma			23.87

V(pc−d1)=600v

χ^2/ndf	95.53	/	63
Constant			2140.
Mean			77.22
Sigma			25.38

V(pc−d1)=700v
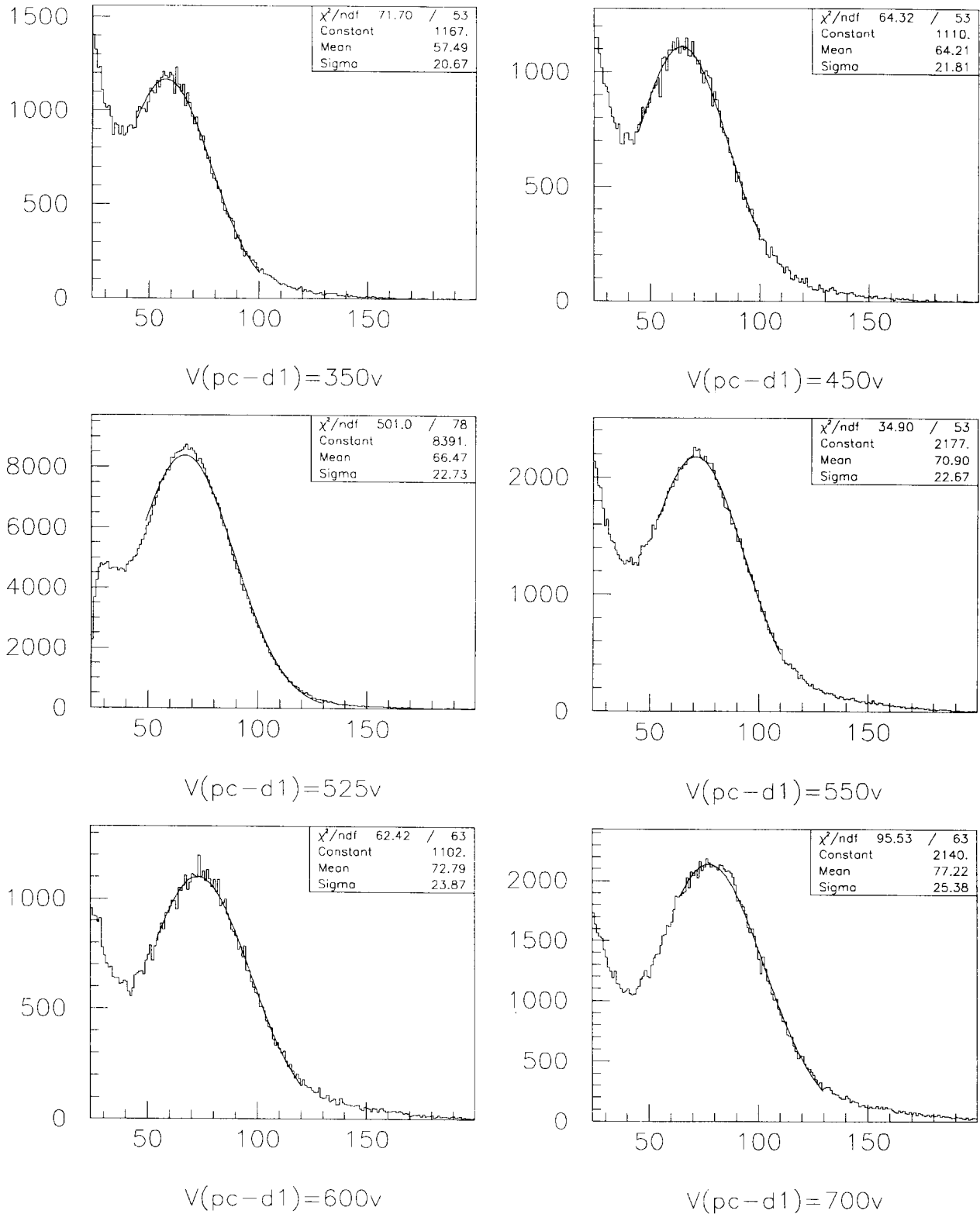
Figure 7: Single-electron amplitude distributions for different photocathode -first dynode potential.

TDC 1bin=0.5ns V(d1−grnd)=1050v. Diff.V(pc−d1).LED−−Neg.polar.

χ^2/ndf	8699.	/	16
Constant	5592.		
Mean	426.9		
Sigma	2.536		

V(pc−d1)=350v

χ^2/ndf	2200.	/	10
Constant	7080.		
Mean	421.1		
Sigma	1.685		

V(pc−d1)=450v

χ^2/ndf	1507.	/	14
Constant	0.1395E+05		
Mean	422.6		
Sigma	2.009		

V(pc−d1)=525v

χ^2/ndf	2867.	/	12
Constant	0.2785E+05		
Mean	420.3		
Sigma	1.619		

V(pc−d1)=550v

χ^2/ndf	362.2	/	12
Constant	0.1361E+05		
Mean	419.8		
Sigma	1.857		

V(pc−d1)=600v

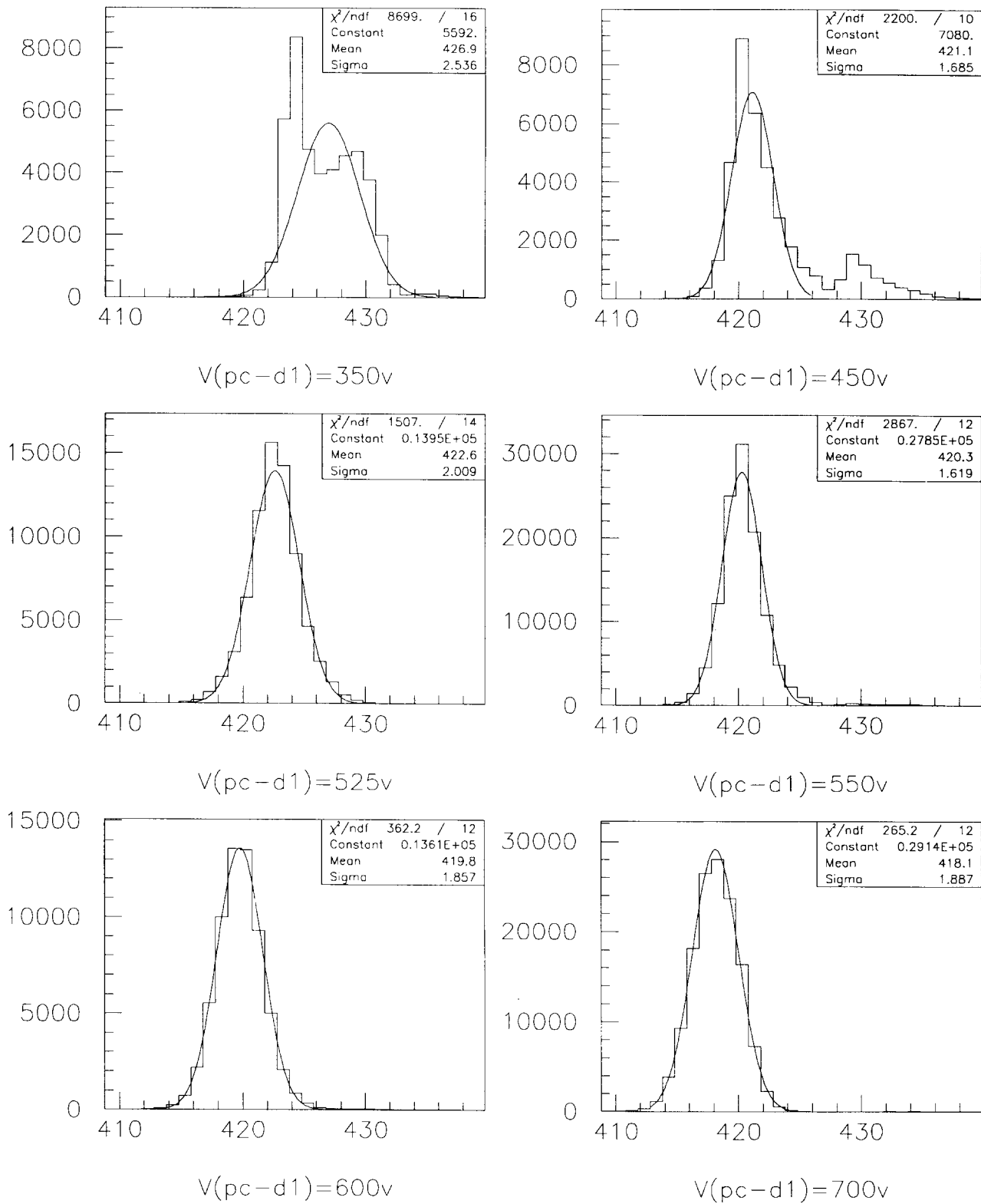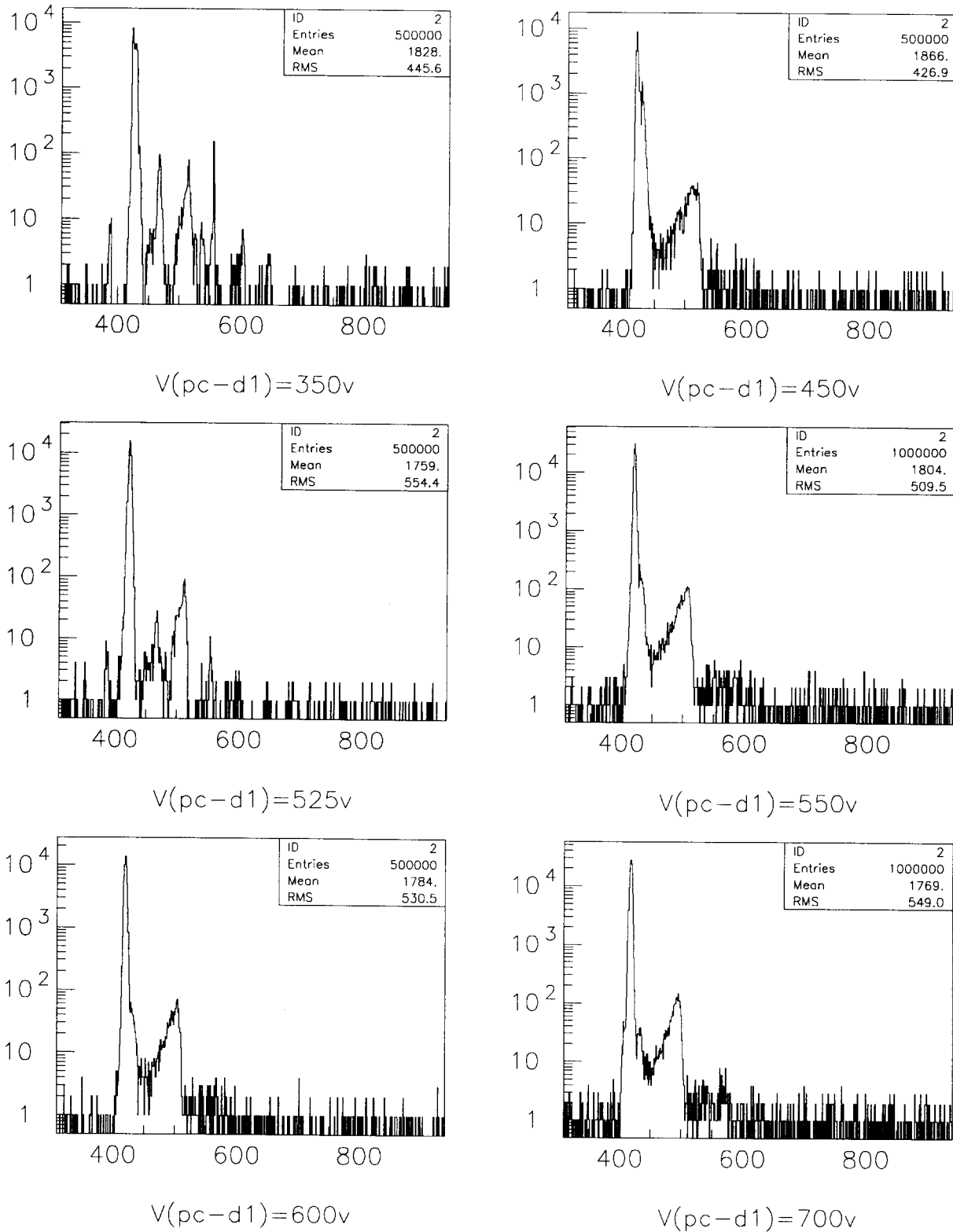| χ^2/ndf	265.2	/	12
Constant	0.2914E+05		
Mean	418.1		
Sigma	1.887		

V(pc−d1)=700v

Figure 8 : Transit time distributions for different photocathode-first dynode potential.

TDC 1bin=0.5ns V(d1−grnd)=1050v. Diff.V(pc−d1).LED−−Neg.polar.

V(pc−d1)=350v

V(pc−d1)=450v

V(pc−d1)=525v

V(pc−d1)=550v

V(pc−d1)=600v

V(pc−d1)=700v

Figure 9: Transit time distributions with afterpulses for different photocathode-first dynode potential.
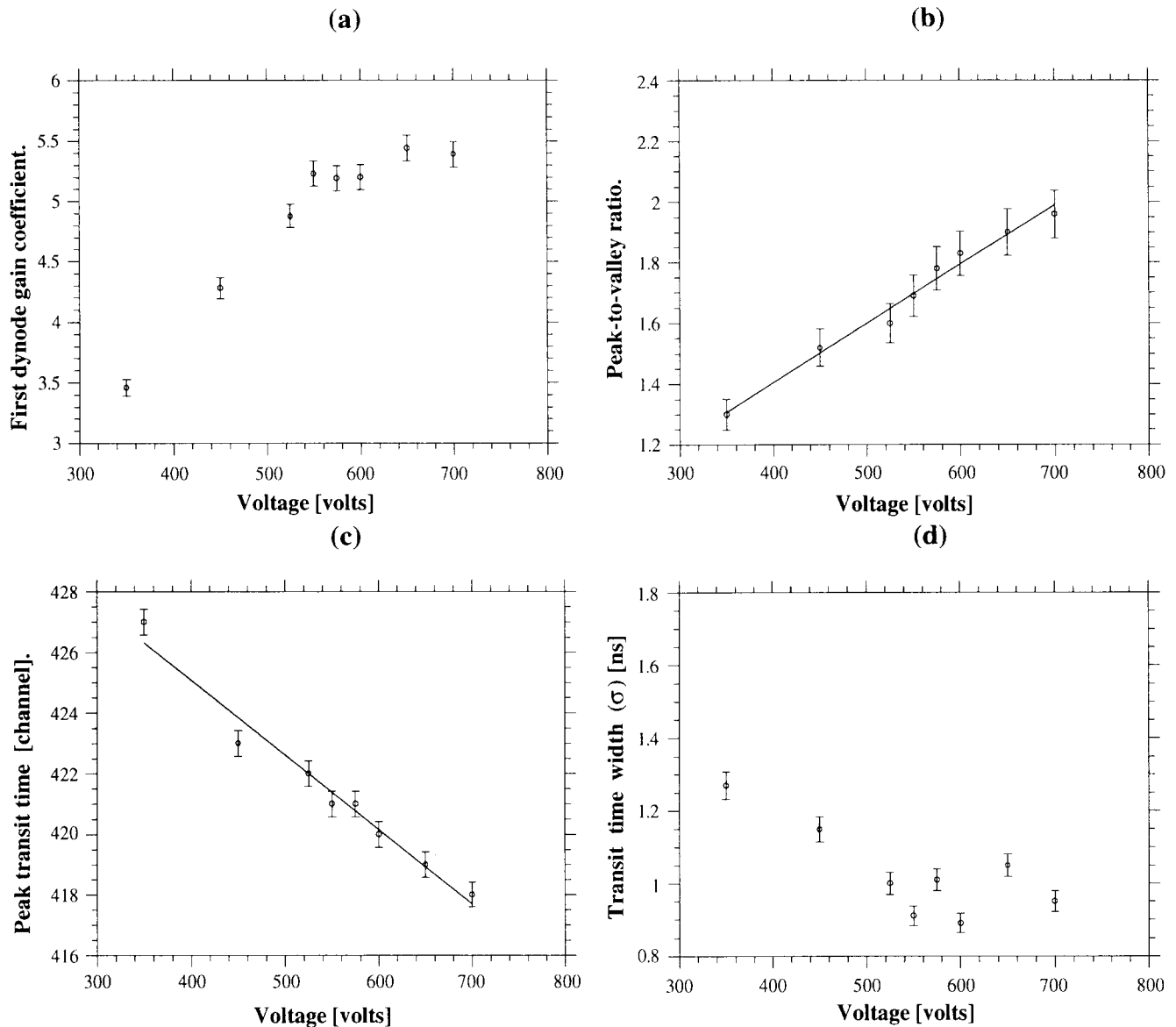
(a)

(b)

(c)

(d)

Figure 10 : Main parameters of EMI versus the voltage between the photocathode and the first dynode:

    a) (mean peak position/width)^2 (pedestal subtracted) : this parameter for single photoelectron regime is dominated by the gain coefficient of the first dynode;

    b) peak-to-valley ratio;

    c) main peak position in transit time distribution;

    d) width of the transit time distribution.

All parameters after V(pc-d1) = 550V change rather slowly, that indicates that the voltage between photocathode and first dynode less than 550 V is not enough to create a proper electric field to collect photoelectrons to the first dynode. In the range 550-700 V one can see a slow rise of the peak-to-valley ratio: by increasing V(pc-d1), we improve the collecting conditions for the photoelectrons. We also see a systematic decrease of the position of the main peak in transit time distribution, due to an increase of the electric field inside of the PM bulb.

4. Transit time distribution.

The main peak in the transit time distribution plot, shows the regular gaussian shape when the voltage between photocathode and first dynode is larger than 500 volts. Using data from plot (d) on figure10, we estimated the width of the main peak as $\sigma = (1.0 \pm 0.1)$ ns.

5. Multiple photoelectrons spectrum.

Knowing the generator amplitude corresponding to one single photoelectron response (from the measurement with a long width of a generator pulse), we increased the LED generator amplitude and investigated the multiple photon response of the EMI PM. The resulting plot is presented in figure 11 with the fit of an exponential function (to describe a left part of the distribution) and 6 gaussians with $q_i = Nq_1$ and $\sigma_i = \sigma_1\sqrt{N}$, where N= 1, 2, ... 6 (like for the figure 5). Parameters P1-P8 on the plot are : P7, P8 correspond to fit of exponential function and P1-P6 are proportional to the probabilities of emitting 1 to 6 photoelectrons. They follow to the Poisson distribution :

$$P(n) = \exp(-x)\,\frac{x^n}{n!} \qquad \text{with x=1.94}$$

EMI Green PD. Start from generator

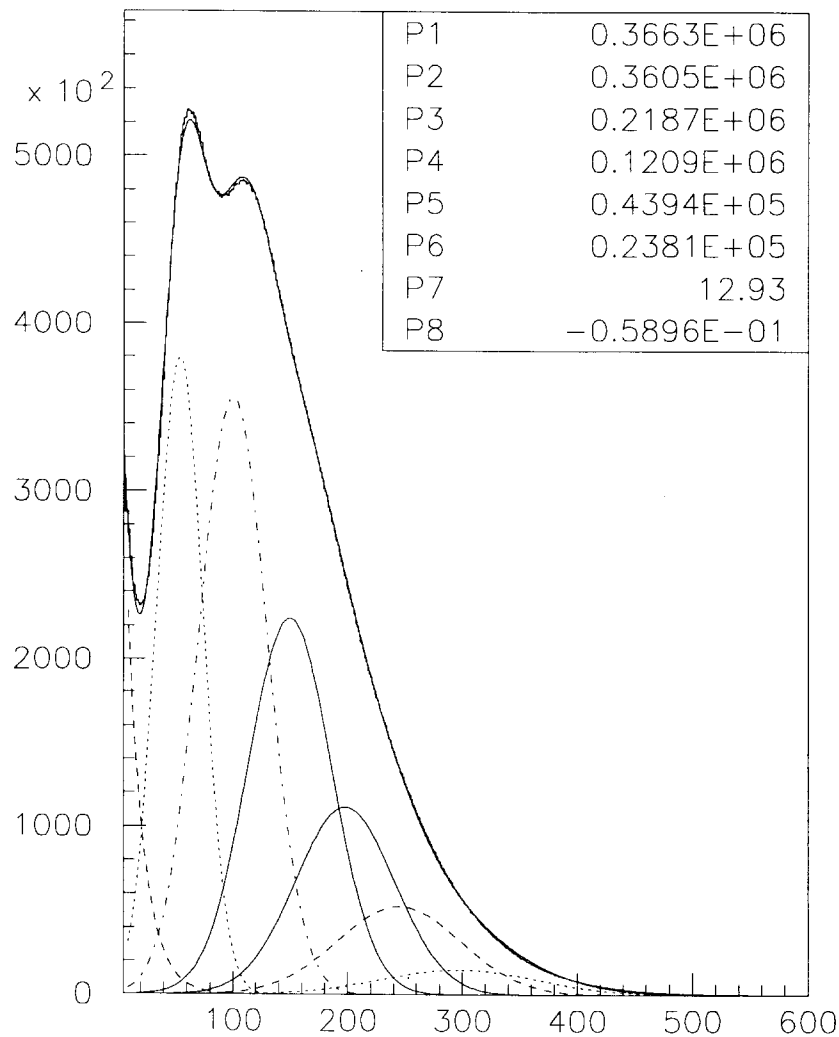|	
P1	0.3663E+06
P2	0.3605E+06
P3	0.2187E+06
P4	0.1209E+06
P5	0.4394E+05
P6	0.2381E+05
P7	12.93
P8	−0.5896E−01

Figure 11 : Multiple photoelectron amplitude distribution.

6. Spectra with a lot of photoelectrons (linearity).

We measured also a response from the EMI PM when the number of photoelectrons is larger than 10, by increasing the amplitude of the LED generator pulse. For each measurement we had a

regular gaussian amplitude distribution. Fitting it we obtained a mean peak position and a width(σ). After that a parameter - (mean peak position/width)^2 was calculated, which corresponds to the number of photoelectrons emitted from the photocathode. The result of these measurements is shown on figure 12 as the number of photoelectrons vs the mean peak position (ADC channel). One can see a satisfactory linearity of the PM, when the number of photoelectrons changes from 10 up to 200. So we checked the possibility to use the EMI PM both in the single photoelectron regime and with a big amount of light.
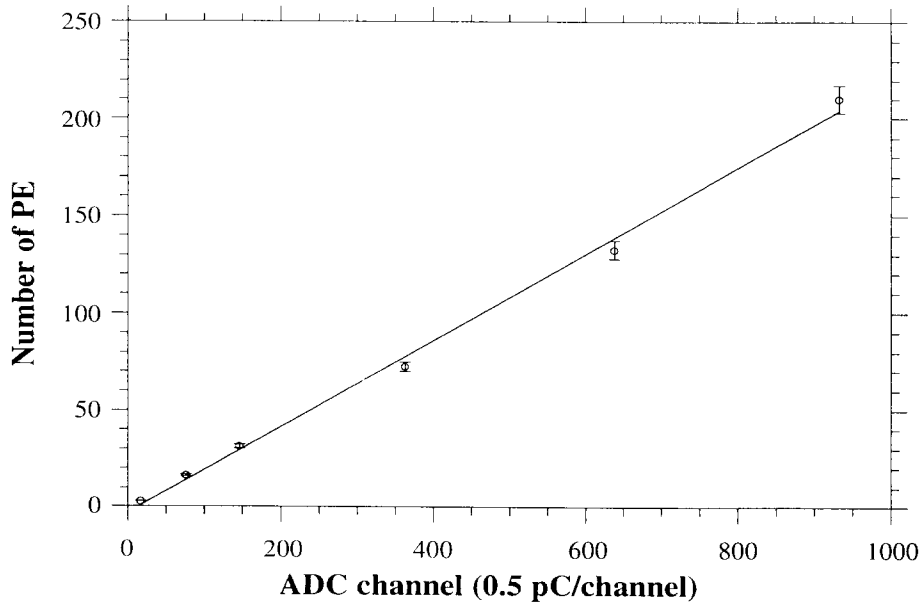

Figure 12 : Amplitude linearity.

7. Afterpulses.

Some additional measurements were done to understand what parameters are more important for afterpulses. For each measurement two values were calculated: N_{main} - is the number of events corresponding the main peak in the time distribution ($\pm 5\ \sigma$ from the main peak position) and N_{aftp} - is the number of events within a time window 100 ns after the main time window. The ratio N_{main}/N_{aftp} was chosen as a parameter to describe the deposit of the afterpulses. These ratios were obtained for:

1) different voltages between the photocathode and first dynode (V(pc-d1)) at fixed voltage between first dynode and ground (V(d1-grnd)=1050V) in the single photoelectron regime (figure 13 - a);

2) different V(d1-grnd) at fixed V(pc-d1) =550V, the threshold being changed to keep it at 0.1 times the single photoelectron peak for different V(d1-grnd):

(figure 13 - b) for the single photoelectron regime;

(figure 13 - c) for measurements with a mean number of photoelectrons about 10;

3) different thresholds at fixed V(d1-grnd)=1100V and V(pc-d1)=550V in the single photoelectron regime:

(figure 13 - d) as a function of the ratio of a threshold to peak position (pedestal was subtracted).

For fig.13-a and 13-b we added the information about measured charge (from corresponding amplitude distributions) to demonstrate how to renormalize the anode signal when V(d1-grnd) and V(pc-d1) are changing.
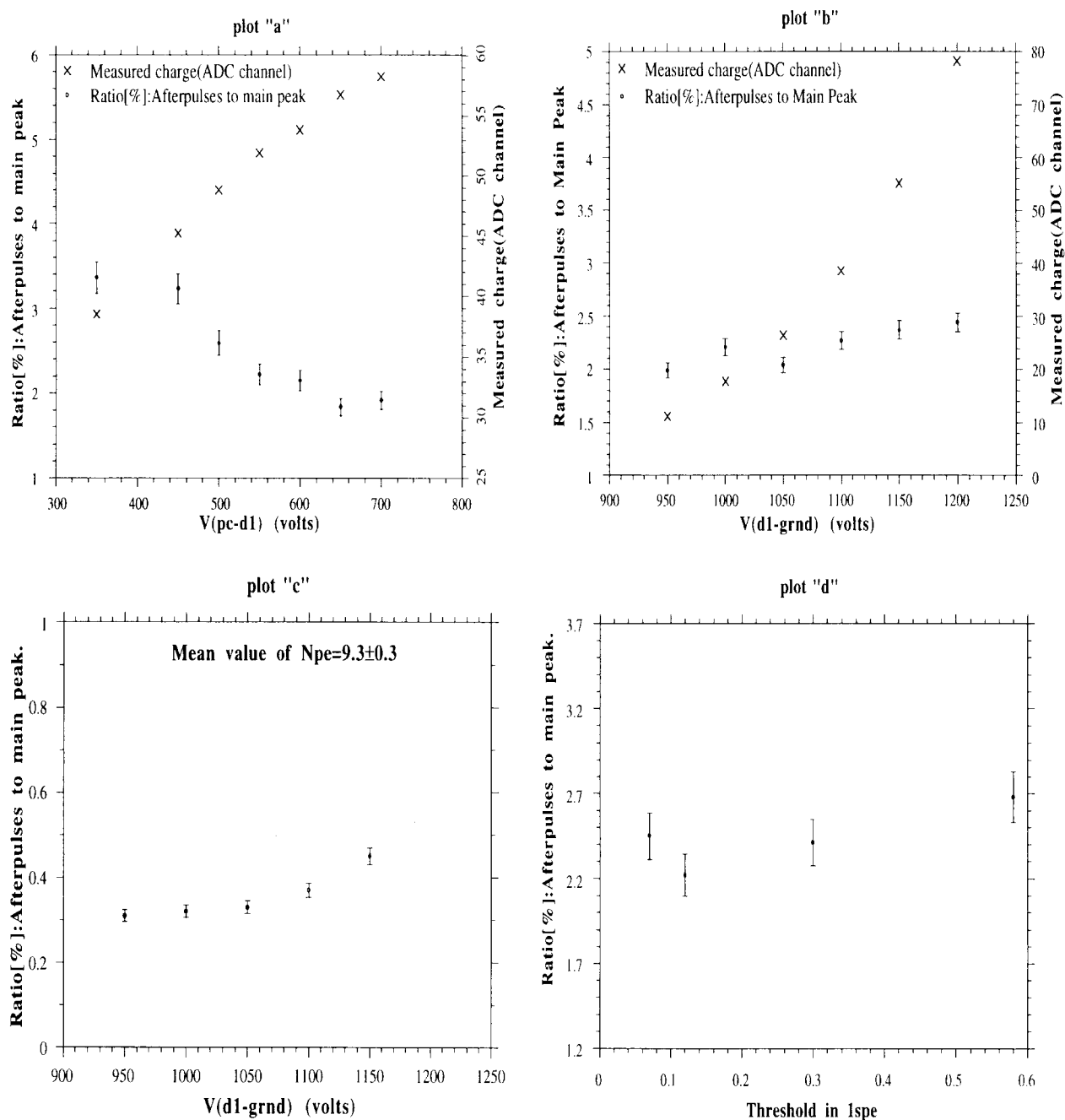
Figure 13 : Afterpulses versus different parameters.

The results of these measurements permit us to make the following conclusions:

1. afterpulses decrease with increasing of number of photoelectrons emitted from the photocathode, due to the decrease of the probability to miss a photoelectron (remind here again that we used classical TDC in our measurements);

2. afterpulses do not change dramatically when changing V(pc-d1) and V(d1-grnd) from 350V up to 700 V and from 950 V up to 1200 V respectively;

3. even in the single photoelectron regime, afterpulses practically do not depend on the output signal threshold, at least when a threshold changes from 0.1 up to 0.6 of the mean value of single photoelectron peak position;

4. afterpulses are mainly located within a time window of 25 ns, which is itself delayed after the main peak about 45 ns (see figure 9).

8. Decay time of the scintillators.

With the EMI and another PM, HP 2020, the time parameters of scintillators (Gd-free and Gd-loaded) were measured. A small quartz box with dimensions 8 x 8 x 50 mm^3 was filled with scintillator. On the top of the box a ^{207}Bi source was placed. The box had optical contact with the HP 2020 . The distance between the box and the EMI-PM was chosen to obtain the single electron regime for the EMI. The amplitude distributions were measured for both PM. Signals from HP 2020 gave the trigger for EMI amplitude and time analyses. Time distributions of both PM were measured with a LED to demonstrate that time parameters of PM are much faster than those of the scintillator. Figure 14 shows the corresponding ADC and TDC spectra for both PM.
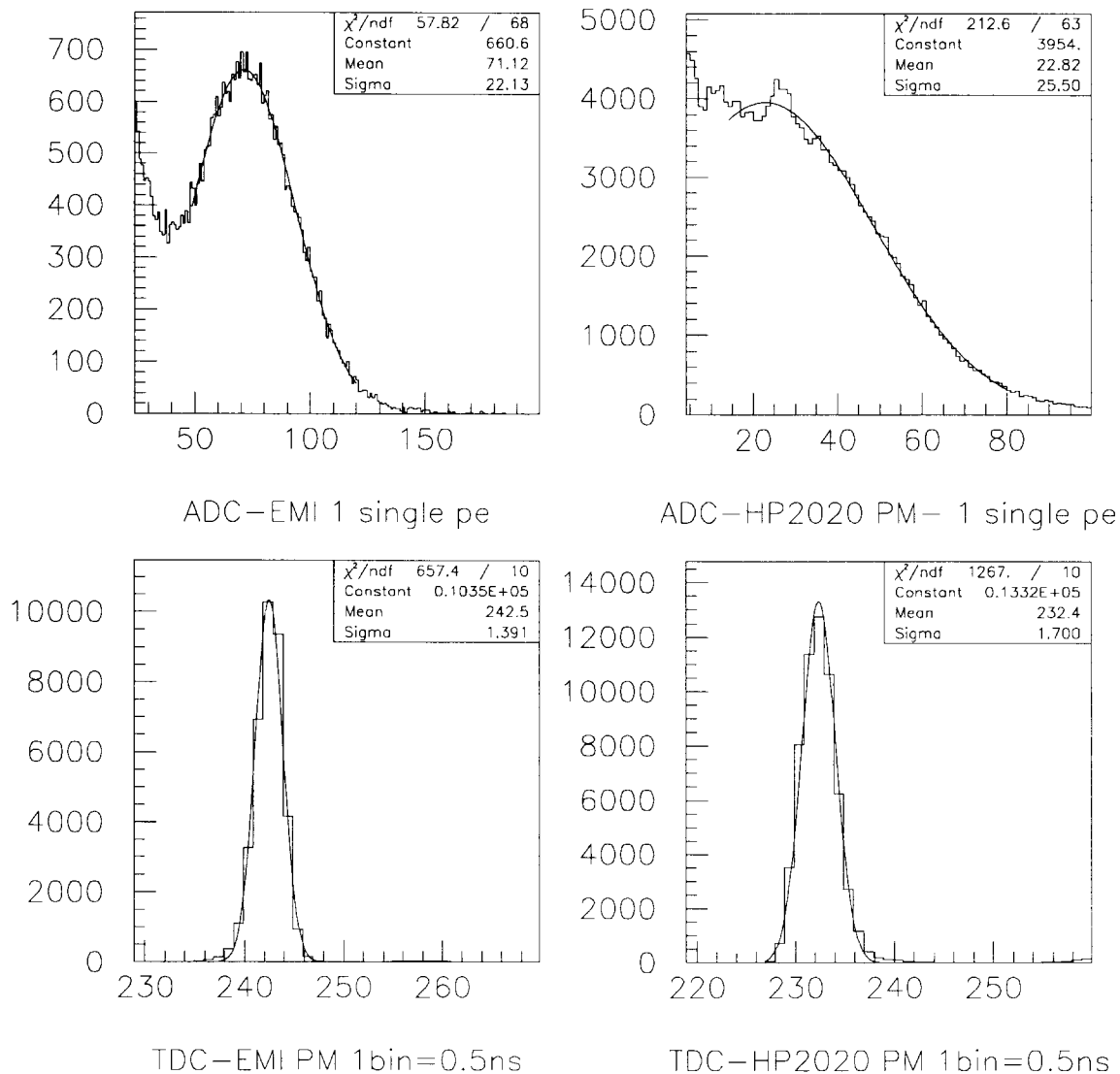

Figure 14: ADC and TDC distributions of both EMI-9351 and HP 2020.

In figure 15 and 16 we present the results of time-constant measurements for both scintillators (gadolinium-free and gadolinium-loaded).
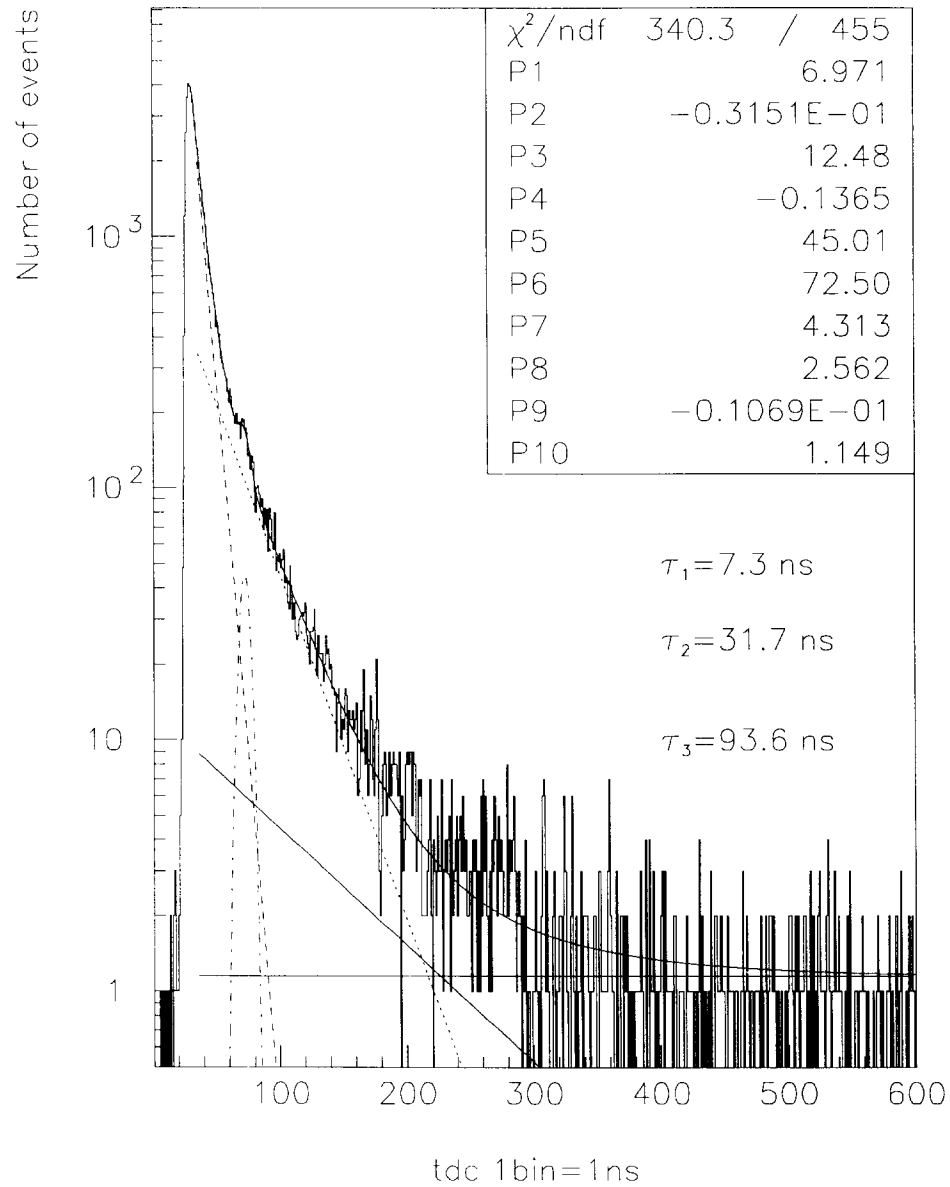

Figure 15: Time-constant measurements for gadolinium-free scintillator.

χ^2/ndf	833.9 / 556
P1	8.452
P2	$-0.4141E-01$
P3	16.80
P4	-0.2469
P5	169.8
P6	68.83
P7	3.932
P8	3.734
P9	$-0.1027E-01$
P10	2.782

$\tau_1 = 4.0$ ns

$\tau_2 = 24.2$ ns

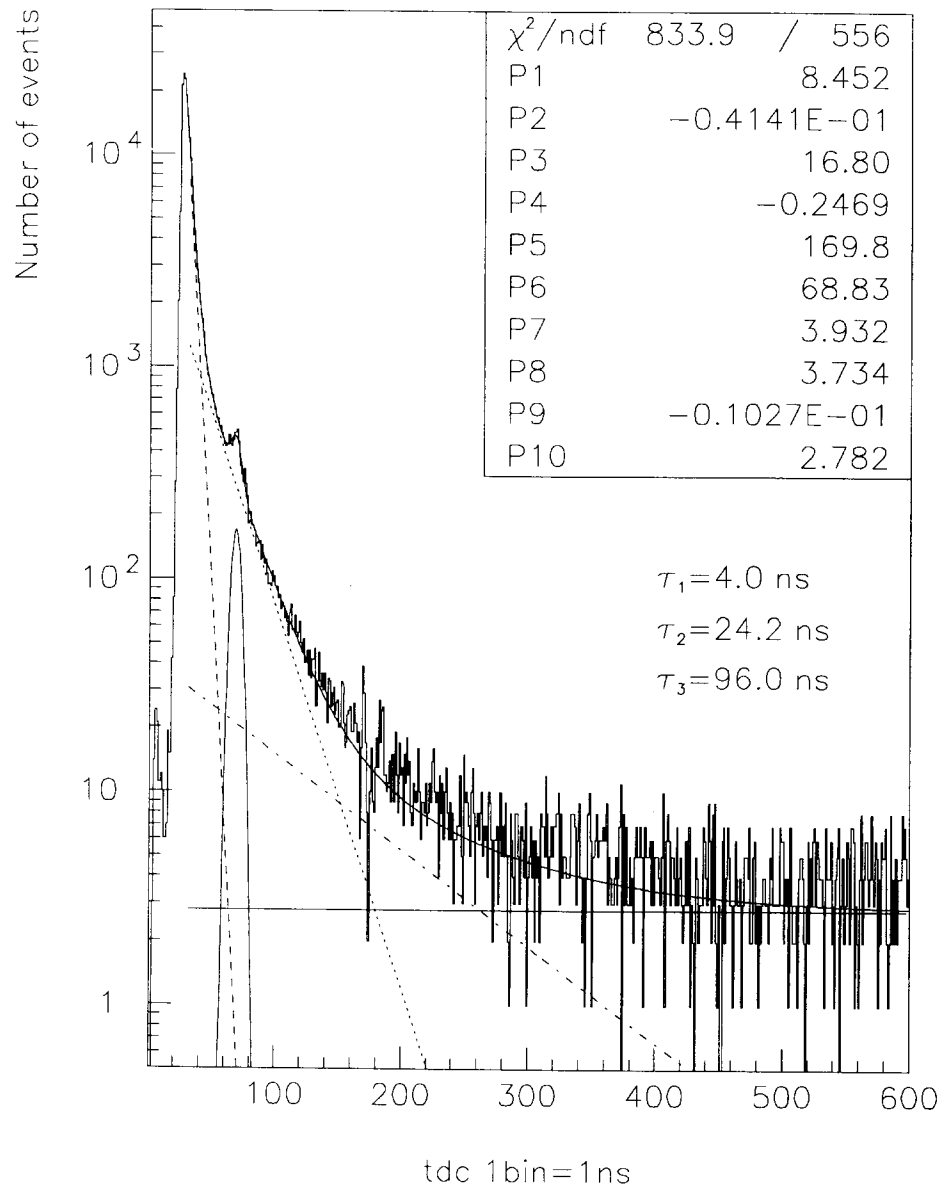$\tau_3 = 96.0$ ns

Number of events

tdc 1bin=1ns

Figure 16 : Time-constant measurements for gadolinium-loaded scintillator.

A fit with three exponentials (to describe time constants of a scintillator) and a gaussian (for afterpulses) was done for both figures. The results of the fit are (they are also presented on figures):

- For the gadolinium-free scintillator, the time constants are :

$$\tau_1 = (7.3 \pm 0.4) \text{ ns} ; \qquad \tau_2 = (31.7 \pm 1.6) \text{ ns} \quad \tau_3 = (93.6 \pm 4.7) \text{ ns}$$

The corresponding probabilities are:

$$Y_1 = (70 \pm 4)\% \qquad Y_2 = (28 \pm 1)\%. \qquad Y_3 = (2 \pm 0.1)\%$$

- For the gadolinium-loaded scintillator, the time constants are :

$$\tau_1 = (4.0 \pm 0.2) \text{ ns} ; \qquad \tau_2 = (24.2 \pm 1.2) \text{ ns} . \quad \tau_3 = (96.0 \pm 4.8) \text{ ns}$$

The corresponding probabilities are:

$$Y_1 = (72 \pm 4)\% \qquad Y_2 = (26 \pm 1)\%. \qquad Y_3 = (2 \pm 0.1)\%$$

Conclusions

The tests performed on EMI showed us that this tube suits well the purposes of CHOOZ experiment, mainly due to :

a) low dark curent noise rate;

b) good single-electron response;

c) narrow single-photoelectron transit time distribution;

d) good linearity up to 2 V for anode output signals.

Note also that the glass of the tube has a low contamination of radioactive materials. This last point is very important for a low background experiment like CHOOZ.

Acknowledgement

We thank the Thorn EMI and HAMAMATSU societies for their help and for fruitful discussions. We are waiting for a new PM from HAMAMATSU (R5912), which must have much better peak-to-valley ratio than R4558. We thank also M.Sené for his help and advice.

---

[1] Proposal to search for neutrino vacuum oscillations to $\Delta m^2 = 10^{-3} \text{ eV}^2$ using a 1 km baseline reactor neutrino experiment NIM.....

[2] See reference 1.

[3] See reference 1.

[4] Performances of large cathode area phototube for underground physics applications. G. Rannucci, R. Cavalletti, P. Inzani and S. Schöner. INFN/AE-92/09.

[5] Characterisation and magnetic shielding of the large cathode area PMT's used for the light detection system of the prototype of the solar neutrino experiment Borexino. G. Rannucci et al. NIM A 337 (1993) 211-220.

[6] Data sheet from Thorn EMI.R/P 069 Voltage Divider Design.